PASJ: Publ. Astron. Soc. Japan **63**, 23–30, 2011 February 25

Astrometry of Galactic Star-Forming Region Onsala 1 with VERA: Estimation of Angular Velocity of Galactic Rotation at the Sun

Takumi NAGAYAMA,[1] Toshihiro OMODAKA,[2] Akiharu NAKAGAWA,[2] Toshihiro HANDA,[3]
Mareki HONMA,[1] Hideyuki KOBAYASHI,[1] Noriyuki KAWAGUCHI,[1] and Takeshi MIYAJI[1]
[1]*Mizusawa VLBI Observatory, National Astronomical Observatory of Japan, 2-21-1 Osawa, Mitaka, Tokyo 181-8588*
[2]*Graduate School of Science and Engineering, Kagoshima University, 1-21-35 Kôrimoto, Kagoshima, Kagoshima 890-0065*
[3]*Institute of Astronomy, The University of Tokyo, 2-21-1 Osawa, Mitaka, Tokyo 181-0015*
takumi.nagayama@nao.ac.jp

(Received 2010 June 18; accepted 2010 December 1)

Abstract

We conducted the astrometry of H_2O masers in the Galactic star-forming region Onsala 1 (ON 1) with the VLBI Exploration of Radio Astrometry (VERA). We measured a trigonometric parallax of 0.404 ± 0.017 mas, corresponding to a distance of 2.47 ± 0.11 kpc. ON 1 appears to be located near the tangent point at a Galactic longitude of 69°.54. We estimated the angular velocity of the Galactic rotation at the Sun (the ratio of the Galactic rotation velocity at the Sun to the distance from the Sun to the Galactic center) to be $\Omega_0 = \Theta_0/R_0 = 28.7 \pm 1.3\,\mathrm{km\,s^{-1}\,kpc^{-1}}$ using the measured distance and proper motion of ON 1. This value is larger than the IAU recommended value of $(220\,\mathrm{km\,s^{-1}}/8.5\,\mathrm{kpc}) = 25.9\,\mathrm{km\,s^{-1}\,kpc^{-1}}$, but consistent with other results recently obtained with the VLBI technique.

Key words: astrometry: — ISM: individual (Onsala 1) — masers (H_2O)

1. Introduction

Very Long Baseline Interferometry (VLBI) astrometry is an important method for measuring the structure of the Milky Way Galaxy. By accurately measuring the position of the source and its time variation, the distance and proper motion of the source could be determined directly. VLBI astrometry at 10 μas accuracy of the Galactic H_2O and CH_3OH maser sources with the VLBI Exploration of Radio Astrometry (VERA) and with the Very Long Baseline Array (VLBA) accurately determined the distance at the kpc-scale with an error of less than 10% (see, e.g., Hachisuka et al. 2006; Xu et al. 2006; Honma et al. (2007)).

The Galactic constants, the distance from the Sun to the Galactic center (R_0) and the Galactic rotation velocity at the Sun (Θ_0), are major parameters necessary to the study of the structure of the Galaxy. The rotation curve of the Galaxy and all kinematic distances of the sources in the Galaxy are directly based on the Galactic constants. Although the International Astronomical Union (IAU) has recommended giving values of $R_0 = 8.5$ kpc and $\Theta_0 = 220\,\mathrm{km\,s^{-1}}$ since 1985, numerous recent studies reveal different values from the IAU values (e.g., Reid et al. 2009).

However, an observational estimation of the Galactic constants is difficult. This is because observational estimations of the Galactic constants are affected by several independent assumptions about motions: the peculiar motion of the source, systemic noncircular motions of both the source and the LSR due to the spiral arm and the nonaxisymmetric potential of the Milky Way Galaxy, and the relative motion of the Sun to the LSR (Reid et al. 2009; McMillan & Binney 2010). To minimize these effects, we should observe many sources located in various regions in the Milky Way Galaxy.

The tangent point where the Galactic rotation vector of the source is parallel to the line of sight is a kinematically unique position in the Milky Way Galaxy. In the case where the source is located at this point and in a circular motion, the proper motion of the source depends only on the Galactic rotation of the Sun, Θ_0. Therefore, we can estimate Θ_0 from the measured proper motion. We can also estimate R_0 from the measured source distance, since the tangent point, the Sun, and the Galactic center make a right triangle. Sato et al. (2010) measured the parallactic distance of W 51 Main/South, which is located near the tangent point, and estimated $R_0 = 8.3 \pm 1.1$ kpc using this simple geometry. If the source is not located at the tangent point, but near there, we can estimate the ratio of Galactic constants, Θ_0/R_0 (the angular velocity of the Galactic rotation at the Sun, Ω_0), as described in section 4. The value of this ratio is a constraint on the estimate of one of the Galactic constants from the other. Although the IAU gives recommended values of the Galactic constants, at least one of them should be revised, if the ratio is to be inconsistent with the observed value.

The radial velocity of the source located at the tangent point is equal to the terminal velocity. It is defined as the extreme velocity on any line of sight at $b \simeq 0°$, and described as $v_{\mathrm{term}} = \Theta - \Theta_0 \sin l$, where Θ is the Galactic rotation velocity of the source. Therefore, we selected those sources whose radial velocities are close to the terminal velocity. One of these sources, Onsala 1 (ON 1), is a massive star-forming region located at the Galactic coordinates of $(l, b) = (69°.54, -0°.98)$. The radial velocity of ON 1 is close to the terminal velocity. The radial velocity observed in molecular lines is $12 \pm 1\,\mathrm{km\,s^{-1}}$ (Bronfman et al. 1996; Pankonin et al. 2001). The terminal velocity at $l = 69°.54$, $14\,\mathrm{km\,s^{-1}}$, is derived from the IAU recommended value of $\Theta_0 = 220\,\mathrm{km\,s^{-1}}$, and assuming flat

rotation ($\Theta = \Theta_0$); it is $15 \pm 5\,\mathrm{km\,s^{-1}}$ in the l–v diagram of Dame, Hartmann, and Thaddeus (2001). The distance of ON 1 was measured to be $2.57^{+0.34}_{-0.27}$ kpc by 6.7 GHz CH_3OH maser astrometry with the EVN (Rygl et al. 2010). VLBI maps of the H_2O masers have been reported by Nagayama et al. (2008). They found that ON 1 has two clusters of H_2O masers (WMC 1 and WMC 2) separated by $1\farcs6$.

In the present study, we report on our successful determination of the parallax of ON 1 with VERA. This is a first step of estimating the Galactic constants and the angular velocity of Galactic rotation at the Sun using VERA.

2. Observations and Reductions

We observed H_2O masers in the star-forming region ON 1 with VERA at 11 epochs during the period of ~ 2 yr. The epochs are as follows (day of year): 245, 256, 290, 309, 360 in 2006, 046, 091, 129, 223 in 2007, and 020, 202 in 2008. At each epoch, the H_2O 6_{16}–5_{23} maser at a rest frequency of 22.235080 GHz in ON 1 and a position-reference source J2010+3322 were simultaneously observed in a dual-beam mode for ~ 10 hr. The typical on-source integration time was 6 hr for both ON 1 and J2010+3322. J2010+3322 is listed in VLBA Calibrator Survey 2 (VCS2: Fomalont et al. 2003). J2010+3322 was detected with a peak flux density of 100–130 mJy in each epoch. The separation angle between ON 1 and J2010+3322 is $1\fdg85$. The instrumental phase difference between the two beams was measured continuously during observations by injecting artificial noise sources into both beams (Honma et al. 2008a). Left-hand circular polarization signals were sampled with 2-bit quantization and filtered with the VERA digital filter unit (Iguchi et al. 2005). The data were recorded onto magnetic tapes at a rate of 1024 Mbps, providing a total bandwidth of 256 MHz, which consists of 16×16 MHz IF channels. One IF channel was assigned to ON 1, and the other fifteen IF channels were assigned to J2010+3322. Correlation processing was carried out on a Mitaka FX correlator. The frequency and velocity resolutions for ON 1 were 31.25 kHz and $0.42\,\mathrm{km\,s^{-1}}$, respectively.

Data reduction was conducted using the NRAO Astronomical Image Processing System (AIPS). An amplitude calibration was performed using the system noise temperatures during the observations. For phase-referencing, a fringe fitting was made using the AIPS task FRING on J2010+3322 with a typical integration time of 2 min. The solutions of the fringe phases, group delays, and delay rates were obtained every 30 s. These solutions were applied to the data of ON 1 in order to calibrate the visibility data. Phase and amplitude solutions obtained from self-calibration of J2010+3322 were also applied to ON 1. Visibility phase errors caused by the Earth's atmosphere were calibrated based on GPS measurements of the atmospheric zenith delay, which occurs due to tropospheric water vapor (Honma et al. 2008b). After the calibration, we made spectral-line image cubes using the AIPS task IMAGR around masers with 1024×1024 pixels of size 0.05 milliarcsecond (mas). The typical size of the synthesized beam was 1.3 mas $\times$ 0.9 mas with a position angle of $-40°$. The rms noise for each image was approximately 0.1–1 Jy beam^{-1}. We adopted a signal-to-noise ratio of 7 for image detection.

In the single-beam VLBI imaging of ON 1 (without phase-referencing to the J2010+3322 in the other beam), group delays solved on J2025+3343 in the same beam were applied. Fringe fitting was done using one of the brightest emissions at an LSR velocity of $14.9\,\mathrm{km\,s^{-1}}$ in ON 1, and the solutions were applied to all velocity channels. The data reductions for single-beam imaging that we followed are the same as those of previous Japanese VLBI network observations of ON 1 (Nagayama et al. 2008).

3. Results

3.1. Overall Properties of H_2O Masers in ON 1

Figure 1 shows the scalar-averaged cross-power spectra of ON 1 H_2O masers at intervals of about half a year. They were obtained with the Mizusawa–Iriki baseline and averaged for the total observational time. There are low-velocity components ($v_{\mathrm{LSR}} = -7$ to $17\,\mathrm{km\,s^{-1}}$) near the systemic velocity of ON 1 ($v_{\mathrm{LSR}} = 12 \pm 1\,\mathrm{km\,s^{-1}}$: Bronfman et al. 1996), and blue-shifted ($v_{\mathrm{LSR}} = -57$ to $-32\,\mathrm{km\,s^{-1}}$) and red-shifted ($v_{\mathrm{LSR}} = 55$ to $70\,\mathrm{km\,s^{-1}}$) high-velocity components. Most of the low-velocity components were detected over a period of one year. The high-velocity components are time-variable, and not persistent for more than half a year.

We detected 28 H_2O maser features for more than two epochs. Figure 2 shows the distributions and internal motions

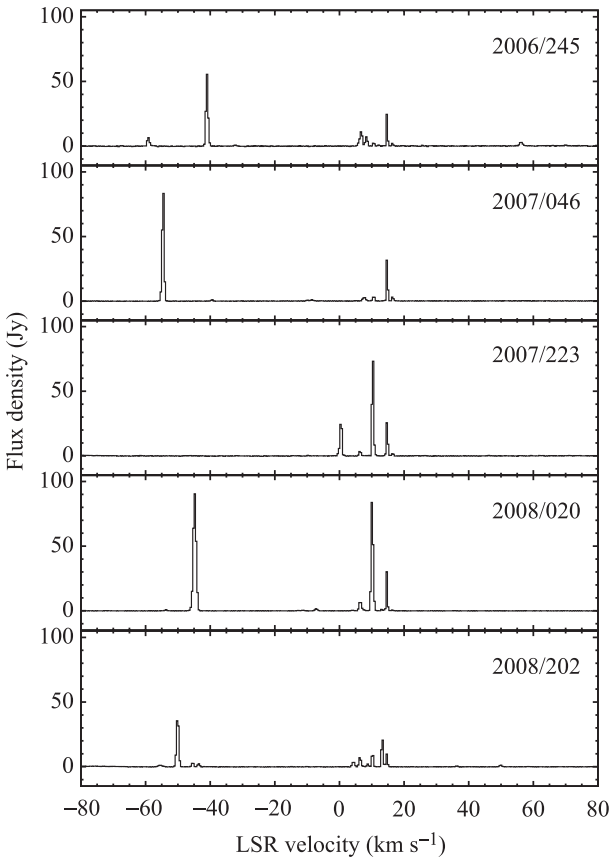

Fig. 1. Scalar-averaged cross-power spectra of the ON 1 H_2O masers obtained with the Mizusawa–Iriki baseline.

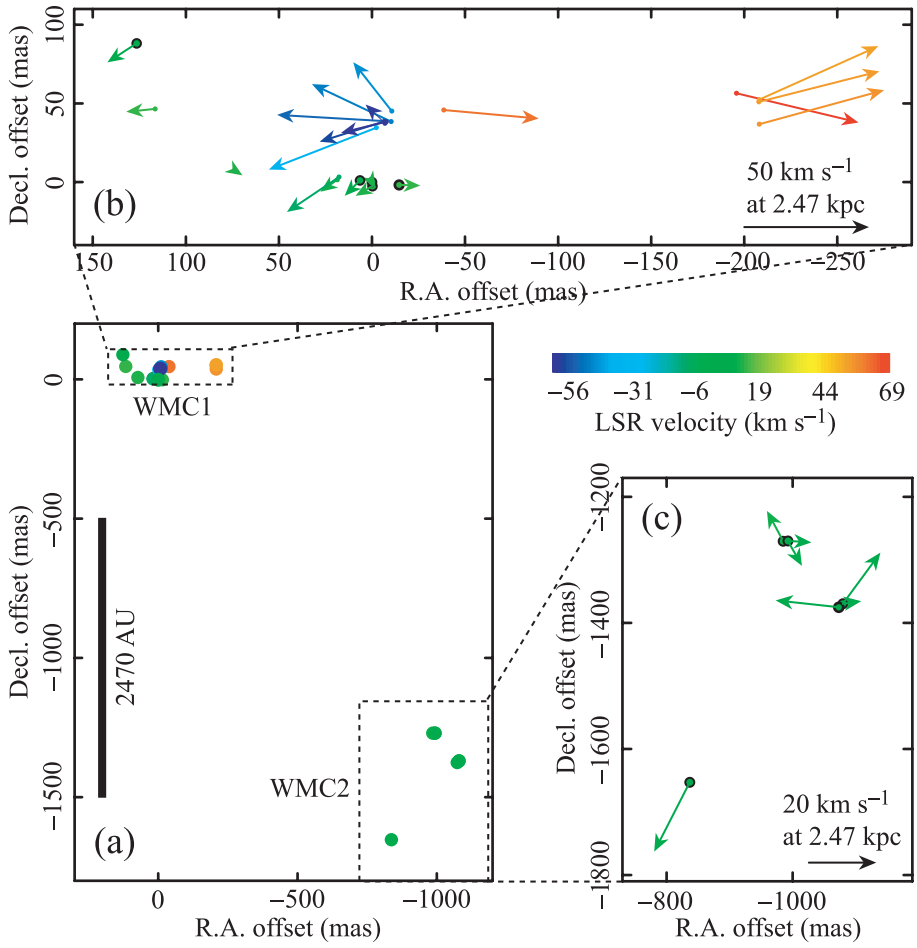

Fig. 2. (a) Distributions of H_2O masers in ON 1. The color index denotes the LSR velocity range of −56.8 to 69.6 km s^{-1}, where 28 features are located. The origin of map is located at the position of the reference maser feature at $v_{\rm LSR} = 14.9$ km s^{-1}: $(\alpha, \delta)_{\rm J2000.0} = (20^{\rm h}10^{\rm m}09^{\rm s}.20454, 31°31'36''.1012)$ in 2006/245. (b), (c) Close-ups to the two maser clusters (WMC 1 and WMC 2) with internal proper-motion vectors. The maser features used for determination of the parallax and proper motion are marked with black circles.

of these features. The masers are distributed over $\sim 1'' \times 2''$ area, which is consistent with those detected by the previous VLBI observations (Nagayama et al. 2008). There is the difference in the time intervals of the epochs between the present and previous observations. By observing at shorter time intervals of 1–2 months, the number of the maser features by which we can trace the internal motions in the present observations increased to twice the previous one. ON 1 has two clusters of H_2O maser features located at $(x, y) \simeq (0''.0, 0''.0)$ and $(-0''.9, -1''.4)$, where x and y are the relative positions in the equatorial coordinate system. They were named water-maser cluster 1 (WMC 1) and WMC 2 by Nagayama et al. (2008), respectively.

The internal motions of WMC 1 exhibit a bipolar outflow structure in the east–west direction. The blue- and red-shifted features show a high expansion velocity of $\simeq 70$ km s^{-1} in the three-dimensional velocity. The low-velocity features with $v_{\rm LSR} = -7$ to 17 km s^{-1} show a low expansion velocity of $\simeq 10$ km s^{-1}. In previous observations, the blue- and red-shifted features were distributed ~ 200 mas apart within two small regions of approximately 15 mas × 15 mas, and others were not detected outside of these regions (Nagayama et al. 2008). They are two clusters of blue-shifted features around $(x, y) \simeq (-5, 45)$ mas and red-shifted around $(-200, 50)$ mas in figure 2b. Nagayama et al. (2008) suggest that a driving source of H_2O masers is located near to the midpoint between these two clusters. However, we have lately detected a new red-shifted feature at $(x, y) \simeq (-40, 45)$ mas. Therefore, the driving source would be located in between the new red-shifted feature and the cluster of the blue-shifted features. In WMC 2, only the low-velocity features ($v_{\rm LSR} = 6$ to 14 km s^{-1}) were detected. Their internal motions did not show any systematic feature, and thus the masers in WMC 2 are not likely to originate from WMC 1. We confirmed that there are two driving sources of H_2O masers in ON 1.

3.2. *Parallax and Proper Motion*

The absolute motions of H_2O masers to an extragalactic source for the position reference are expressed by the sum of a linear motion and the trigonometric parallax. We conducted monitoring observations of H_2O masers for ~ 2 yr, and their absolute motions were successfully obtained relative to a position-reference source, J2010+3322. Figure 3 shows positional variations of one of the brightest maser features at

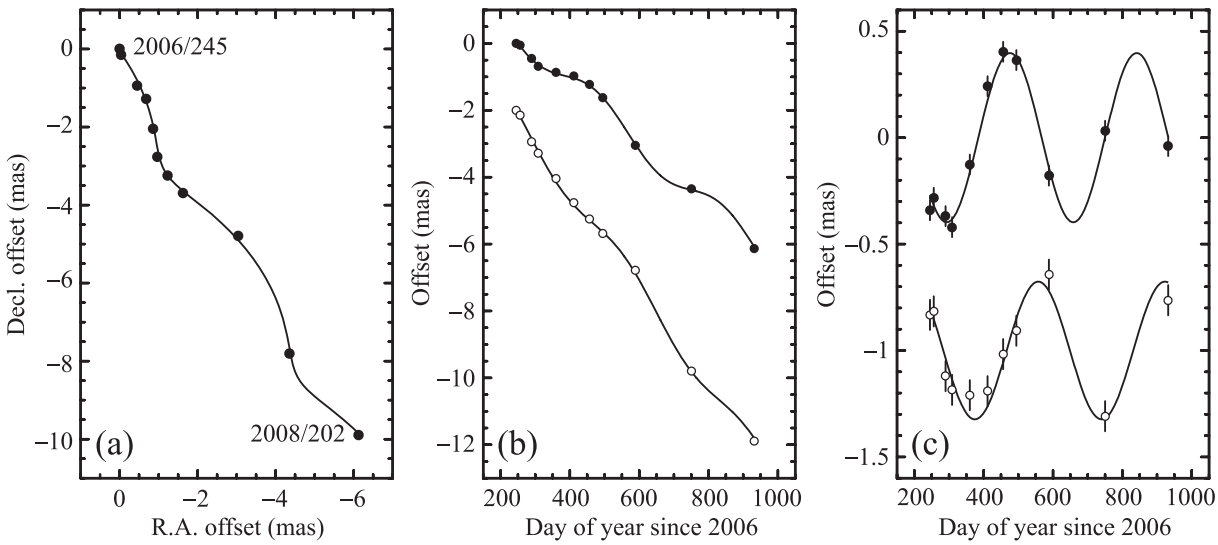

Fig. 3. Parallax and proper motion data and fits for the maser feature of $v_{\rm LSR} = 14.9\,{\rm km\,s^{-1}}$. (a) Positions on the sky with first and last epochs labeled. The solid line indicates the parallax and proper-motion fit. (b) x (filled circles) and y (open circles) position offsets versus time. The solid line indicates the parallax and proper-motion fit. The y data have been offset from the x data for clarity. (c) Same as (b) panel, except that the proper-motion fit has been removed, allowing the effects of only the parallax to be seen.

Table 1. Best-fit values of the parallaxes and proper motions for ten H_2O maser features in ON 1.*

ID	$\Delta\alpha$ (mas)	$\Delta\delta$ (mas)	$v_{\rm LSR}$ (km s^{-1})	Detected epochs	π (mas)	$\mu_\alpha\cos\delta$ (mas yr^{-1})	μ_δ (mas yr^{-1})
1	126.5	88.1	7.7	11111111100	0.389 ± 0.036	-2.65 ± 0.09	-5.58 ± 0.12
2	6.5	1.1	10.2	00011111111	0.428 ± 0.025	-2.73 ± 0.05	-5.44 ± 0.08
3	0.0	0.0	14.9	11111111111	0.407 ± 0.021	-3.42 ± 0.03	-5.30 ± 0.04
4	-0.2	-2.6	14.4	01111111110	0.420 ± 0.041	-3.32 ± 0.05	-5.21 ± 0.07
5	-14.6	-1.8	16.5	11111111111	0.382 ± 0.031	-3.89 ± 0.07	-4.94 ± 0.09
6	-836.8	-1653.0	10.6	11111111111	0.421 ± 0.066	-3.20 ± 0.09	-5.02 ± 0.12
7	-985.1	-1270.3	14.0	11111111000	0.390 ± 0.055	-3.51 ± 0.10	-4.08 ± 0.14
8	-994.3	-1269.9	6.4	11111100000	0.382 ± 0.057	-3.71 ± 0.15	-3.15 ± 0.21
9	-1073.2	-1375.1	8.5	11111110000	0.399 ± 0.039	-2.05 ± 0.11	-3.72 ± 0.16
10	-1079.9	-1369.5	7.3	00111111110	0.416 ± 0.065	-2.51 ± 0.15	-4.58 ± 0.20
		Combined fit			0.404 ± 0.012		
		Average				-3.10 ± 0.18	-4.70 ± 0.24

* Columns (2), (3): Offsets relative to the positon of the maser feature at $v_{\rm LSR} = 14.9\,{\rm km\,s^{-1}}$: $(\alpha, \delta)_{\rm J2000.0} = (20^{\rm h}10^{\rm m}09\overset{\rm s}{.}20454, 31^\circ31'36\overset{''}{.}1012)$ in 2006/245. Column (4): LSR velocity. Column (5): Detected epochs: "1" for detection and "0" for nondetection. Column (6): Parallax estimates. Columns (7), (8): Motions on the sky along the right ascension and declination.

$v_{\rm LSR} = 14.9\,{\rm km\,s^{-1}}$. The positional variations show systematic sinusoidal modulation with a period of 1 yr, caused by the parallax.

In order to derive the parallax and proper motion, we used the positions of ten maser features detected over a period of half a year. We conducted a combined parallax fit, in which the positions of ten features were fitted simultaneously with one common parallax, but different proper motions and position offsets for individual spots. For this fit, we used errors of 0.057 mas in right ascension and 0.082 mas in declination, in quadrature to the formal fitting errors. This resulted in χ^2 per degree of freedom values of unity for both the right ascension and the declination data. The resulting parallax is 0.404 ± 0.012 mas. Table 1 gives the results of the combined parallax fit.

To check the consistency among the parallax motions for individual maser features, we also estimated the parallax individually. In table 1, we also show the obtained parallaxes using individual fittings for their maser features. The obtained parallaxes of ten maser features are consistent with each other, from 0.382 to 0.428 mas, and give a similar result of 0.404 ± 0.012 mas.

Combining the results of ten maser features can lead the parallax uncertainty to an underestimation, in the case where the measurements of different maser features are correlated with each other. Randomlike errors, such as map noise and

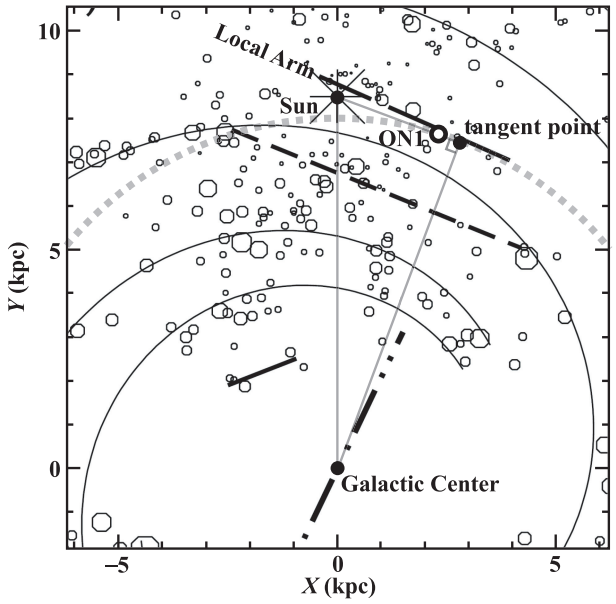

Fig. 4. Position of ON 1 in the Milky Way Galaxy. The background is the four spiral-arm structures (Russeil 2003). The thick lines sketched by Russeil (2003) show the local arm feature (long dashed line), the bar orientation and length (dashed-dot-dot line) from Englmaier and Gerhard (1999), the expected departure from a logarithmic spiral arm observed for the Sagittarius–Carina arm (short dashed line), and a feature certainly linked to the three kpc arm (solid line).

the maser feature structure variation, would not be correlated with each other. However, systemic errors (e.g., from the correlator model or the atmosphere) would affect all maser features at one epoch in a very similar way. A conservative approach would prove that the uncertainty is not reduced even if combined fittings of ten maser features are made. In this approach, the uncertainty would be estimated to be 0.021 mas from the smallest uncertainty of the ID 3 maser feature. However, the results of ten maser features are not entirely correlated, since the obtained parallaxes from individual fittings do not have completely the same value. Therefore, we estimated the final uncertainty of the parallax, taking an average of the uncertainties of 0.012 mas and 0.021 mas, and obtain 0.404 ± 0.017 mas, which we choose this value as the parallax of ON 1.

The obtained parallax corresponds to a source distance of 2.47 ± 0.11 kpc. This distance is consistent with the 6.7 GHz CH_3OH maser parallax corresponding to $2.57^{+0.34}_{-0.27}$ kpc that was measured by Rygl et al. (2010), but was 2 times accurately obtained. Figure 4 shows the position of ON 1 in the Milky Way Galaxy, which is determined from the distance of 2.47 ± 0.11 kpc, a longitude of $l = 69.^{\circ}54$ and $R_0 = 8.5$ kpc. ON 1 appeared to be located on the Local arm and near to the tangent point at $l = 69.^{\circ}54$.

The absolute-proper motion of a maser feature is the sum of the internal motion of the maser feature, the Galactic rotation, the solar motion, and the peculiar motion of the source. All motions, except for the internal motion, are common to all maser features. Therefore, the average of the absolute proper motions of the maser features should give the systemic proper motion of the whole source, if the internal motions are well randomized. We consider that this is valid for ON 1, because the averaged radial velocity of ten maser features is 11.1 km s^{-1}, which is consistent with the systemic radial velocity derived from the associated molecular cloud ($v_{\rm LSR}$ $= 12 \pm 1$ km s^{-1}: Bronfman et al. 1996). The absolute proper motions of ten maser features range from -3.89 to -2.05 mas yr^{-1} in right ascension and from -5.58 to -3.15 mas yr^{-1} in declination. From the average (the arithmetic mean) of these values, the systemic proper motion of ON 1, $(\mu_\alpha \cos\delta, \mu_\delta) = (-3.10 \pm 0.18, -4.70 \pm 0.24)$ mas yr^{-1}, is derived where the error is the standard error. Although there is a difference of approximately 1 mas yr^{-1} between the averaged proper motions of WMC 1 and WMC 2, it would be the relative stellar motion, since WMC 1 and WMC 2 are associated with different sources. Averaging the motions of multiple sources can also help to determine the systemic motion of ON 1. We compared this to the proper motion obtained by Rygl et al. (2010). Rygl et al. (2010) measured the proper motions of ON 1 using two background sources, J2003+3034 and J2009+3049, and obtained different proper motions between them because of their apparent movements. Our derived systemic proper motion is close to the proper motion obtained using J2009+3049.

We converted the proper motion of $(\mu_\alpha \cos\delta, \mu_\delta)$ $= (-3.10 \pm 0.18, -4.70 \pm 0.24)$ mas yr^{-1} to one with respect to LSR using the solar motion in the traditional definition of $(U_\odot, V_\odot, W_\odot) = (10.3, 15.3, 7.7)$ km s^{-1}. In previous studies for the astrometry of Galactic maser sources, the solar motion of $(U_\odot, V_\odot, W_\odot) = (10.00, 5.25, 7.17)$ km s^{-1} based on the HIPPARCOS satellite data (Dehnen & Binney 1998) was widely used. However, Schönrich, Binney, and Dehnen (2010) suggested that the value of $V_\odot$ determined by Dehnen and Binney (1998) is underestimated by ~ 7 km s^{-1}, and showed a value that is close to the value of the traditional definition used in this study. Using Galactic coordinates of ON 1, $(l, b) = (69.^{\circ}54, -0.^{\circ}98)$, the proper motion with respect to LSR projected to the direction of l and b was calculated to be $(\mu_l, \mu_b) = (-6.00 \pm 0.22, 0.69 \pm 0.20)$ mas yr^{-1}. This proper motion corresponds to a velocity of $(v_l, v_b) = (-70.2 \pm 2.6, 8.1 \pm 2.3)$ km s^{-1}.

4. Discussion

As shown in section 1, the source at the tangent point has a kinematically unique property, and one of the key objects of the study on the kinematics and geometry of the Milky Way Galaxy. Due to a symmetric geometry, the radial velocity of a source at the tangent point with perfect circular motion is equal to the terminal velocity.

The radial velocity of ON 1 observed in molecular lines is 12 ± 1 km s^{-1} (Bronfman et al. 1996; Pankonin et al. 2001). The terminal velocity at $l = 69.^{\circ}54$ is 15 ± 5 km s^{-1} (Dame et al. 2001). They are the same within error limits. This suggests that ON 1 is located at the tangent point. In the case where the source is located exactly at the tangent point and in a circular motion, the source, the Sun, and the Galactic center make a right triangle, and the proper motion of the source on the sky depends only on the Galactic rotation of the Sun.

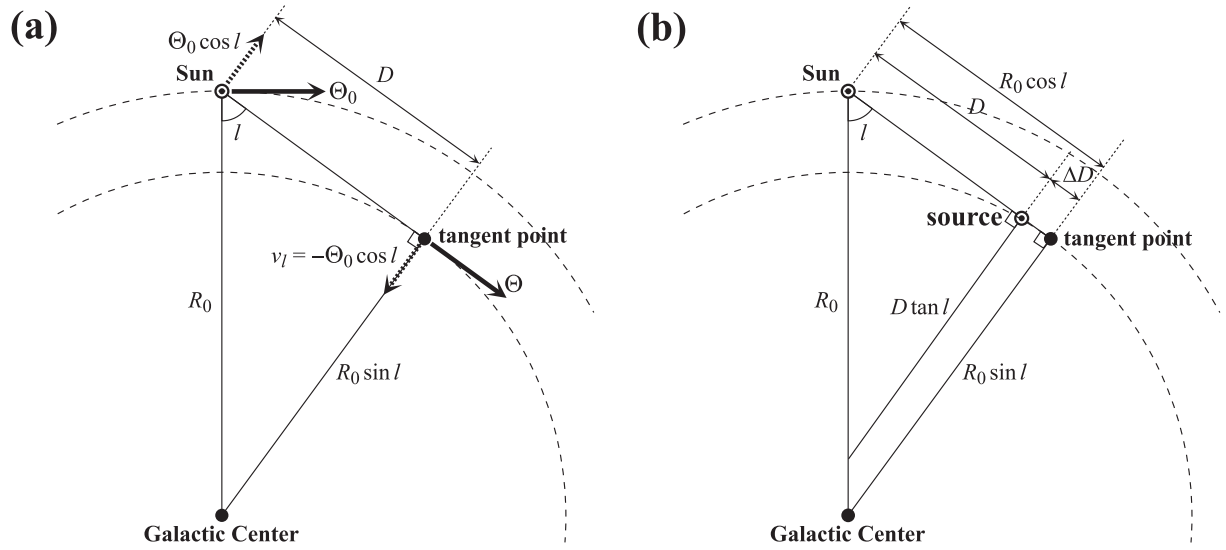

Fig. 5. Geometry of the Galactic center, the Sun, the tangent point, and the source. (a) Geometry in the case where the source is located at the tangent point. (b) Geometry in the case where there is an offset between the source and the tangent point.

This geometry is shown in figure 5a. Therefore, R_0 and Θ_0 are determined from the observed distance to the source, D, and the proper motion on the sky along the Galactic plane, v_l, as

$$R_0 = D/\cos l, \tag{1}$$

$$\Theta_0 = -v_l/\cos l. \tag{2}$$

The Galactic constants are estimated to be $R_0 = 7.1 \pm 0.3$ kpc and $\Theta_0 = 201 \pm 7\,\mathrm{km\,s^{-1}}$, respectively, from $D = 2.47 \pm 0.11$ kpc and $v_l = -70.2 \pm 2.6\,\mathrm{km\,s^{-1}}$. These values are approximately 10%–20% smaller than previous values, such as the IAU recommended values of $R_0 = 8.5$ kpc and $\Theta_0 = 220\,\mathrm{km\,s^{-1}}$, the recently estimated of $R_0 = 8.4 \pm 0.6$ kpc and $\Theta_0 = 254 \pm 16\,\mathrm{km\,s^{-1}}$ (Reid et al. 2009), and $R_0 = 8.3 \pm 1.1$ kpc estimated using the parallax measurement of W51 Main/South located near the tangent point (Sato et al. 2010).

However, our estimated R_0 and Θ_0 would not be inconsistent with the previous estimates. This is because our estimation is affected by the ambiguities of the two assumptions: ON 1 is in a circular motion, and is located exactly at the tangent point. We evaluated these effects. Since the velocity deviation of the molecular cloud in ON 1 is estimated to be 3–8 $\mathrm{km\,s^{-1}}$ from the full width at half maximum of the profiles in molecular lines (Zheng et al. 1985; Haschick & Ho 1990; Bronfman et al. 1996), the maser source in ON 1 may have peculiar motion with a similar velocity. If we allow for this peculiar motion of 3–8 $\mathrm{km\,s^{-1}}$, the errors of our estimated R_0 and Θ_0 are over 10%–20%. In the case where we use the IAU recommended values of $R_0 = 8.5$ kpc and $\Theta_0 = 220\,\mathrm{km\,s^{-1}}$, and assume flat rotation, the peculiar motion is estimated to be $(U', V', W') = (7.0 \pm 2.5, -1.8 \pm 1.3, 8.1 \pm 2.3)\,\mathrm{km\,s^{-1}}$ from the measured distance, proper motion, and radial velocity using a method shown in Reid et al. (2009). Here, U' is the velocity component toward the Galactic Center, V' the component in the direction of the Galactic rotation, and W' the component toward the north Galactic pole. In the case where we use other Galactic constants of $R_0 = 8.4$ kpc and $\Theta_0 = 254\,\mathrm{km\,s^{-1}}$ (Reid et al. 2009), the peculiar motion is estimated to be $(U', V', W') = (-3.7 \pm 2.5, -3.2 \pm 1.3, 8.1 \pm 2.3)\,\mathrm{km\,s^{-1}}$. In both cases, the peculiar motion velocity is in the range of the velocity deviation of the molecular cloud. There may be a difference of approximately $5\,\mathrm{km\,s^{-1}}$ between the radial velocity and the terminal velocity, taking their error limits into consideration. If this difference in velocity is due to the offset from the tangent point to ON 1, this offset is estimated to be approximately ± 1.7 kpc. If ON 1 is not located exactly at the tangent point and there is an offset of ± 1.7 kpc between them, the errors of our estimated R_0 and Θ_0 increase to approximately 70%.

Although the estimated values of the Galactic constants are strongly affected by the assumption about the location of the source in the Milky Way Galaxy, we found that the ratio of the Galactic constants, Θ_0/R_0 (the angular velocity of Galactic rotation at the Sun, Ω_0) can be estimated with little ambiguity. In the case where the source is in a circular motion at any position in the Galactic disk, the radial and tangential velocities of the source can be written as

$$v_r = \left(\frac{\Theta}{R} - \frac{\Theta_0}{R_0}\right) R_0 \sin l, \tag{3}$$

$$v_l = \left(\frac{\Theta}{R} - \frac{\Theta_0}{R_0}\right) R_0 \cos l - \frac{\Theta}{R} D. \tag{4}$$

From these equations, the relation between the Θ_0 and R_0 is obtained to be

$$\begin{aligned}\Theta_0 &= \left[-\frac{v_l}{D} + v_r\left(\frac{1}{D\tan l} - \frac{1}{R_0 \sin l}\right)\right] R_0 \\ &= \left[-a_0\mu_l + v_r\left(\frac{1}{D\tan l} - \frac{1}{R_0 \sin l}\right)\right] R_0,\end{aligned} \tag{5}$$

where a_0 is a constant of conversion from a proper motion to

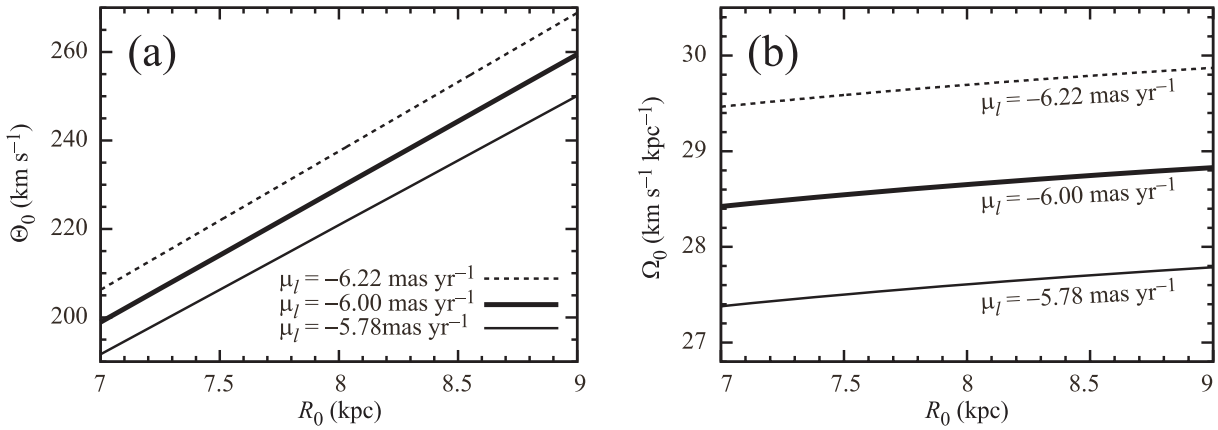

Fig. 6. (a) Relation of R_0 and Θ_0 shown in equation (5). (b) Relation of R_0 and Θ_0/R_0 shown in equation (6).

a linear velocity ($4.74\,\mathrm{km\,s^{-1}\,mas^{-1}\,yr\,kpc^{-1}}$). Equation (5) is graphed in figure 6a using the observed values of $D = 2.47 \pm 0.11\,\mathrm{kpc}$, $\mu_l = -6.00 \pm 0.22\,\mathrm{mas\,yr^{-1}}$, and $v_r = 12 \pm 1\,\mathrm{km\,s^{-1}}$. We found that the slope in figure 6a remains fairly constant at $7 \leq R_0 \leq 9\,\mathrm{kpc}$. The slope yields the ratio Θ_0/R_0, which is described as

$$\frac{\Theta_0}{R_0} = -\frac{v_l}{D} + v_r\left(\frac{1}{D\tan l} - \frac{1}{R_0 \sin l}\right) = -a_0\mu_l + v_r\left(\frac{1}{D\tan l} - \frac{1}{R_0\sin l}\right), \quad (6)$$

Equation (6) is graphed in figure 6b. The ratio is estimated to be $\Theta_0/R_0 = 28.7 \pm 1.3\,\mathrm{km\,s^{-1}\,kpc^{-1}}$ using the above observed values, and $7 \leq R_0 \leq 9\,\mathrm{kpc}$. The error of Θ_0/R_0 depends mainly on that of μ_l. The errors of Θ_0/R_0 that depend on those of v_r and D are ± 0.02 and $\pm 0.05\,\mathrm{km\,s^{-1}\,kpc^{-1}}$, respectively; they can be neglected in this estimation. This is because $D\tan l \simeq R_0 \sin l$ in the case where the source is located near to the tangent point (see figure 5b). We adopted $7 \leq R_0 \leq 9\,\mathrm{kpc}$ in this estimation. This means that ON 1 is located within a range of -0.02–$0.68\,\mathrm{kpc}$ from the tangent point, because the offset from the tangent point is written as $\Delta D = R_0\cos l - D$.

Our estimated ratio, $\Theta_0/R_0 = 28.7 \pm 1.3\,\mathrm{km\,s^{-1}\,kpc^{-1}}$, is close to the value of $27.3 \pm 0.8\,\mathrm{km\,s^{-1}\,kpc^{-1}}$ obtained from the parallax and proper-motion measurements of ON 2 N, which is located on the solar circle (Ando et al. 2011). Our value is consistent with that of $\Theta_0/R_0 = 29.45 \pm 0.15\,\mathrm{km\,s^{-1}}$ estimated from a proper-motion measurement of Sgr A* (Reid & Brunthaler 2004). Reid and Brunthaler (2004) adopted the solar motion in the direction of Galactic rotation of $V_\odot = 5.25\,\mathrm{km\,s^{-1}}$ (Dehnen & Binney 1998). We adopted the solar motion in the traditional definition of $(U_\odot, V_\odot, W_\odot) = (10.3,\ 15.3,\ 7.7)\,\mathrm{km\,s^{-1}}$ (see subsection 3.2). The error of our value depends on that of $V_\odot$, and is estimated to be $\pm 1.4\,\mathrm{km\,s^{-1}\,kpc^{-1}}$ from $V_\odot = 15 \pm 10\,\mathrm{km\,s^{-1}}$. Even if we take account of this error, our value is larger than the IAU recommended value of $220\,\mathrm{km\,s^{-1}}/8.5\,\mathrm{kpc} = 25.9\,\mathrm{km\,s^{-1}\,kpc^{-1}}$.

We can find other sources that are expected to be located at the tangent point from the Arcetri catalog of H_2O masers (Valdettaro et al. 2001). Therefore, we will observe these sources with VERA in order to determine the Galactic constants and the angular rotation velocity of the Galactic rotation at the Sun.

We are grateful to an anonymous referee for valuable comments and suggestions. We give thanks to the staff members of all the VERA stations for their assistances in the observations.

References

Ando, K., et al. 2011, PASJ, 63, 45
Bronfman, L., Nyman, L.-A., & May, J. 1996, A&AS, 115, 81
Dame, T. M., Hartmann, D., & Thaddeus, P. 2001, ApJ, 547, 792
Dehnen, W., & Binney, J. J. 1998, MNRAS, 298, 387
Englmaier, P., & Gerhard, O. 1999, MNRAS, 304, 512
Fomalont, E. B., Petrov, L., MacMillan, D. S., Gordon, D., & Ma, C. 2003, AJ, 126, 2562
Hachisuka, K., et al. 2006, ApJ, 645, 337
Haschick, A. D., & Ho, P. T. P. 1990, ApJ, 352, 630
Honma, M., et al. 2007, PASJ, 59, 889
Honma, M., et al. 2008a, PASJ, 60, 935
Honma, M., Tamura, Y., & Reid, M. J. 2008b, PASJ, 60, 951
Iguchi, S., Kurayama, T., Kawaguchi, N., & Kawakami, K. 2005, PASJ, 57, 259
McMillan, P. J., & Binney, J. J. 2010, MNRAS, 402, 934
Nagayama, T., Nakagawa, A., Imai, H., Omodaka, T., & Sofue, Y. 2008, PASJ, 60, 183
Pankonin, V., Churchwell, E., Watson, C., & Bieging, J. H. 2001, ApJ, 558, 194
Reid, M. J., et al. 2009, ApJ, 700, 137
Reid, M. J., & Brunthaler, A. 2004, ApJ, 616, 872
Russeil, D. 2003, A&A, 397, 133
Rygl, K. L. J., Brunthaler, A., Reid, M. J., Menten, K. M., van Langevelde, H. J., & Xu, Y. 2010, A&A, 511, A2

Sato, M., Reid, M. J., Brunthaler, A., & Menten, K. M. 2010, ApJ, 720, 1055
Schönrich, R., Binney, J., & Dehnen, W. 2010, MNRAS, 403, 1829
Valdettaro, R., et al. 2001, A&A, 368, 845
Xu, Y., Reid, M. J., Zheng, X. W., & Menten, K. M. 2006, Science, 311, 54
Zheng, X. W., Ho, P. T. P., Reid, M. J., & Schneps, M. H. 1985, ApJ, 293, 522